EPJ Web of Conferences **339**, 08002 (2025) https://doi.org/10.1051/epjconf/202533908002
Hard Probes 2024

Direct virtual photon production in Au+Au collision at 27 and 54.4 GeV

Xianwen Bao[1,*] (for the STAR Collaboration)

[1]Key Laboratory of Particle Physics and Particle Irradiation (MOE), Shandong University, Qingdao 266237, China

Abstract. As electromagnetic probes, photons have the advantage of escaping unimpeded from their emission source, allowing them to carry valuable information about the properties and dynamics of the hot quantum chromodynamics (QCD) medium created in heavy-ion collisions. Particularly, the transverse momentum distribution of direct virtual photons emitted from the hot QCD medium exhibits sensitivity to the system temperature. Direction photons from thermal radiation in the low transverse momentum region are expected to be a quark-gluon plasma (QGP) thermometer. However, the photon from hadronic decays make the extraction of the thermal radiation contribution very challenging.

The STAR experiment has recorded large datasets of Au+Au collisions in the Beam Energy Scan Phase-II (BES-II) program, spanning center-of-mass energies of $\sqrt{s_{\rm NN}}$ = 3 - 54.4 GeV. In these proceedings, we present the latest direct virtual photon measurement in Au+Au collisions at $\sqrt{s_{\rm NN}}$ = 27 and 54.4 GeV, including $p_{\rm T}$ differential invariant yields and total yields in different centrality bin. The total yields increase rapidly with increasing $dN_{\rm ch}/d\eta$. Notably, it scales with $(dN_{\rm ch}/d\eta)^{\alpha}$, where $\alpha = 1.46 \pm 0.07$.

1 Introduction

Direct virtual photons play an important role in the study of the QGP. They serve as electromagnetic probes, owing to their ability to escape unimpeded from their emission sources. Direct virtual photons contain prompt photons from initial hard scattering and thermal photons from QGP thermal radiation in heavy ion collision. Because direct virtual photons are produced during all stages of an ultra-relativistic heavy ion collision, they carry information of the properties and dynamics of QGP, such as energy density, temperature and collective motion, integrated over space and time [1] [2].

However, the measurement is challenging due to significant background contributions from hadronic decays. Precise estimation of these backgrounds is essential for accurately determining the thermal radiation originating from QGP.

The PHENIX collaboration reported for the first time the production of direct photons in Au+Au collisions at $\sqrt{s_{\rm NN}}$ = 200 GeV [3]. Subsequently, in 2017, the STAR collaboration reported results on direct virtual photon production using the internal conversion method [4],

*e-mail: baoxianwen@mail.sdu.edu.cn

revealing a discrepancy — nearly a factor of four lower yields than the direct photon yields measured by PHENIX. This difference remains unresolved to date.

In these proceedings, direct virtual photon measurement results are presented at $\sqrt{s_{\rm NN}}$ = 27 and 54.4 GeV in Au+Au collision at different centralities in the STAR experiment and compared to results from the PHENIX and ALICE collaboration, aiming to contribute to a more comprehensive understanding of direct photon production in the QGP [5].

2 Analysis

The data used in this analysis were collected by STAR detector in 2018 (2017) Au+Au collisions at $\sqrt{s_{\rm NN}}$ = 27 (54.4) GeV. STAR detector provides full azimuthal angle ($-\pi < \phi < \pi$) and mid-pseudorapidity ($|\eta| < 1$) acceptance coverage. The average particle ionization energy loss per unit length ($\langle dE/dx \rangle$) and momentum (p) are measured by the time projection chamber (TPC) [6], and the velocity of charged particles is measured by the time of flight (TOF) detector [7]. The electron identification is achieved by combining the $\langle dE/dx \rangle$ and velocity information.

2.1 Dielectron raw signal extraction

For the reconstruction of the dielectron spectrum, the foreground is constructed by pairing electron and positron candidates after removing background contributions. The background is estimated using like-sign pairs, which include correlated and combinatorial background. An acceptance correction is applied to the like-sign pairs, which is estimated using unlike-sign and like-sign pairs from an event-mixing technique [8]. Additionally, dielectrons originating from interaction between the photon and detector material (photon conversion) are rejected by applying a ϕ_V vs. M_{ee} cut, where ϕ_V represents the opening angle of electron pairs. After subtracting the background from the foreground, the raw signal is obtained.

2.2 Efficiency

Efficiency correction, accounting for both electron identification efficiency and electron detection efficiency, is applied to the dielectron raw signal. Here, electron identification efficiency (PID) refers to the efficiency of correctly classifying an already reconstructed track as an electron or positron. Electron detection efficiency encompasses the efficiency of reconstructing and registering the track itself within the detector system. The particle identification efficiency contain $n\sigma_e$ ($\varepsilon_{n\sigma_e}$) and β (ε_β) cut efficiency, which is calculated by selecting pure electron/positron originating from photon conversion [8]. The TPC reconstruction efficiency (ε_{TPC}) is calculated using the embedding technique and the TOF matching efficiency (ε_{TOF})[9] is determined through a data-driven method. Furthermore, the dielectron pair efficiency as shown in Eq. 1, is obtained by multiplying the single track efficiencies of the electron (ε_{e^-}) and positron(ε_{e^+}).

$$\begin{aligned} \varepsilon_{e^{+/-}} &= \varepsilon_{TPC} * \varepsilon_{TOF} * \varepsilon_{n\sigma_e} * \varepsilon_\beta, \\ \varepsilon_{pair} &= \varepsilon_{e^+} * \varepsilon_{e^-}, \end{aligned} \tag{1}$$

2.3 Direct virtual photon extraction

Direct virtual photons are measured via their internal conversion into dielectron pairs, which can be detected by the STAR experiment. However, as mentioned in Sect. 1, there will be

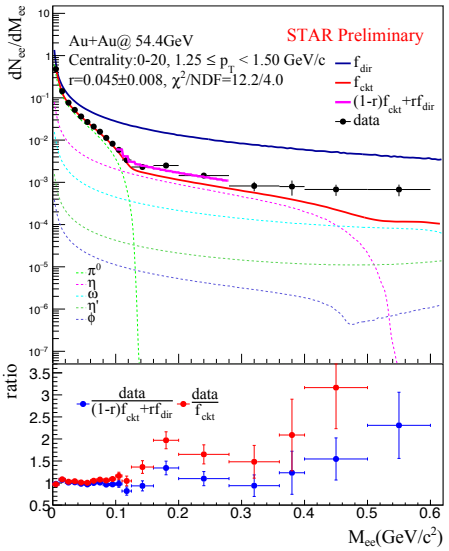

Figure 1. The upper panel show dielectron invariant mass spectrum within STAR acceptance ($p_T^e > 0.2$ GeV, $|\eta^e| < 1$, $|y_{ee}| < 1$) after efficiency correction in Au+Au collisions at $\sqrt{s_{\rm NN}} = 54.4$ GeV in 0-20% centrality. The dashed lines and solid red lines show the contributions from hadronic decays. The pink line is obtained by the two-component fitting. The lower panel shows the ratio of data to cocktail (red solid circles) and data to two-component fit result (blue solid circles).

backgrounds that need to be subtracted in this analysis. The dominant background originate from Dalitz decay of η and π^0, which can be effectively simulated with Monte Carlo, requiring $p_{\rm T}$, mass, ϕ and rapidity distribution as a input for mesons with a dielectron decay. These simulations are normalized using measured hadron yields and $p_{\rm T}$ spectra [10]. The contribution of direct virtual photons to the inclusive dielectron spectrum is very small. Thus, the estimate of the η contribution needs to be very accurate. The η and π^0 spectra are parametrized using Tsallis blast-wave functions, where the parameters are constrained using existing data [12]. The normalization of η is constrained using worldwide data of η/π^0 [11]. It is fixed to 0.470 ± 0.017 for $p_{\rm T} > 5$ GeV/c [13].

The form factor of the virtual photon is similar to that of the η Dalitz decay. However, it deviates significantly from that of the π^0 Dalitz decay around 140 MeV, a region where the π^0 form factor exhibits variation. Thus, the mass distribution between the electron pairs from hadron decay and electron pairs from virtual photons is different, which enables the extraction of direct virtual photon signal via a two-component fit as described by Eq. 2.

$$\frac{dN_{ee}}{dM_{ee}} = r * f_{dir} + (1 - r) * f_{ckt}, \tag{2}$$

where r is the fraction of direct virtual photons to inclusive virtual photons, f_{dir} and f_{ckt} represent direct virtual photon and cocktail mass distribution, respectively. Since the signal and background in this analysis are under STAR acceptance, the proportion of direct photons is extracted by the two-component method which can eliminate the acceptance effect of r by taking the ratio.

The result of two-component fit (fit range: 0.10-0.28 GeV/c^2) is depicted in Fig. 1. Compared with cocktail, data show a slight enhancement attributed to direct virtual photon. We observe that the data over the fit is consistent with unity over the mass range in different centrality and $p_{\rm T}$ bins, which indicates reasonable quality of estimation of cocktail and fitting.

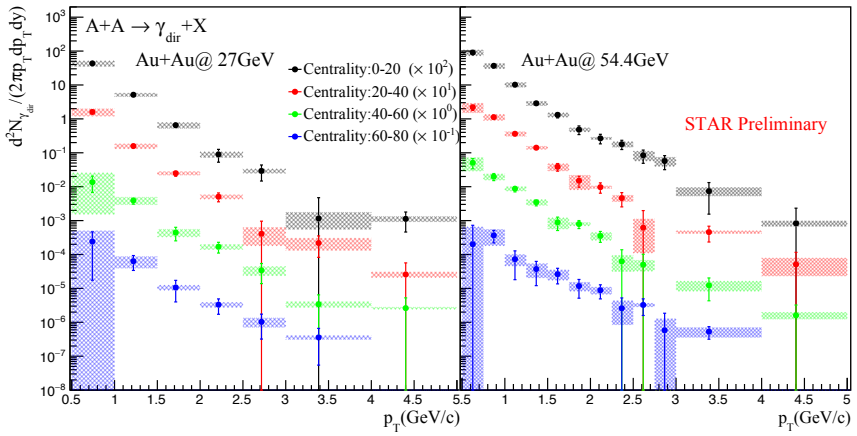

Figure 2. Direct virtual photon transverse momentum spectra in Au+Au collisions at $\sqrt{s_{\rm NN}}$ = 27 (left panel) and 54.4 (right panel) GeV. The $p_{\rm T}$ spectra with different color markers present different centralities cases.

3 Results and discussion

3.1 Direct virtual photon $p_{\rm T}$ spectra and yield

The direct virtual photon transverse momentum spectra in different centralities are shown in Fig. 2. These spectra include prompt and thermal photons, which provide a chance to measure the thermal radiation characteristics and properties of QGP.

STAR presented the direct virtual photon yields in different centralities at $\sqrt{s_{\rm NN}}$ = 200 GeV, which are correlated with $dN_{\rm ch}/d\eta$ [4]. A comparison with theoretical calculations in proton-proton collisions [18] imply that in Au+Au collisions, the direct photons in the transverse momentum range between 1 and 3 GeV/c is dominated by thermal photons. The integrated-p$_T$ spectrum from 1 to 3 GeV/c of direct virtual photon yields at 27 and 54.4 GeV in Au+Au collision are shown in Fig. 3. The STAR data indicate that the direct virtual photon yield exhibits a strong dependence on $dN_{\rm ch}/d\eta$ [15]. But the results difference between PHENIX and STAR are still unresolved. Equation 3 is used to fit direct photon yield from STAR collaboration. The obtained α value is 1.46 ± 0.07.

$$\frac{dN_{\gamma_{dir}}}{dy} = A * (dN_{\rm ch}/d\eta)^{\alpha}. \tag{3}$$

4 Summary

We reported the direct virtual photon transverse momentum spectra in Au+Au collision in different centralities at $\sqrt{s_{\rm NN}}$ = 27 and 54.4 GeV, measured by STAR experiment at RHIC. The direct photon yield reveals a strong dependence on $dN_{\rm ch}/d\eta$. The direct photon yields measured in Au+Au collisions at $\sqrt{s_{\rm NN}}$ = 27, 54.4, and 200 GeV measured by the STAR Collaboration follow a power-law dependence on the charged particle multiplicity with an exponent α = 1.46 ± 0.07. The direct photon yields in Pb+Pb collisions at $\sqrt{s_{\rm NN}}$ = 2.76

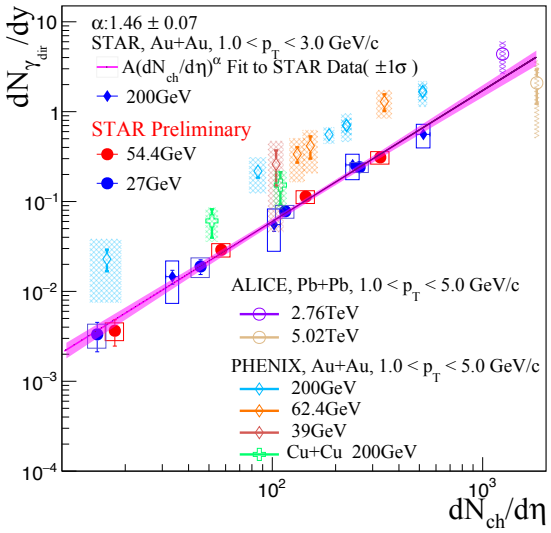

Figure 3. Direct virtual photon yield which integrated in the p_T region of 1.0-3.0 GeV/c. The pink line is obtained by fitting the STAR direct photon yield at $\sqrt{s_{NN}}$ = 27 (blue solid circles), 54.4 (red solid circles), and 200 GeV (blue solid diamonds) direct photon yield from STAR collaboration, pink band indicate the fitting 1σ error. Open circles are the results of ALICE collaboration [16]. Open diamonds and crosses are the results of PHENIX collaboration [17].

and 5.02 TeV measured by the ALICE collaboration are also consistent with this power-law dependence despite the large difference in the collision energies. In the future, we plan to subtract the prompt photon contribution with the help of theoretical calculations, in order to extract the effective temperature of thermal photons. BES-II program provides an excellent opportunity to extend direct photon measurements to lower collision energies corresponding to higher chemical baryon potential.

5 Acknowledgments

The work is partly supported by Shandong Provincial Natural Science Foundation under Grant No. ZR2022JQ03 and ZR2024QA192, and the National Natural Science Foundation of China under Grant No. 12475142.

References

[1] E.V. Shuryak, Quark-Gluon Plasma and Hadronic Production of Leptons, Photons and Psions. Phys.Lett.B 78 (1978) 150. https://doi.org/10.1016/0370-2693(78)90370-2

[2] J. Chen, X. Dong, X. He, H. Huang, F. Liu, X. Luo, et al., Properties of the QCD matter: review of selected results from the relativistic heavy ion collider beam energy scan (RHIC BES) program. Nucl.Sci.Tech. 35 (2024) 12, 214. https://doi.org/10.1007/s41365-024-01591-2

[3] PHENIX Collaboration, Centrality dependence of direct photon production in $\sqrt{s_{NN}}$ = 200GeV Au + Au collisions. Phys.Rev.Lett. 94 (2005) 232301. https://doi.org/10.1103/PhysRevLett.94.232301

[4] STAR Collaboration, Direct virtual photon production in Au+Au collisions at $\sqrt{s_{NN}}$ = 200 GeV. Phys.Lett.B 770 (2017) 451-458. https://doi.org/10.1016/j.physletb.2017.04.050

[5] STAR Collaboration, Temperature Measurement of Quark-Gluon Plasma at Different Stages. arXiv:2402.01998 [nucl-ex]. https://arxiv.org/abs/2402.01998

[6] M. Anderson, J. Berkovitz, W. Betts, R. Bossingham, F. Bieser et al, The Star time projection chamber: A Unique tool for studying high multiplicity events at RHIC. Nucl.Instrum.Meth.A 499 (2003), 659-678. https://doi.org/10.1016/S0168-9002(02)01964-2

[7] STAR Collaboration, Multigap RPCs in the STAR experiment at RHIC. Nucl.Instrum.Meth.A 661 (2012), S110-S113. https://doi.org/10.1016/j.nima.2010.07.086

[8] PHENIX Collaboration, Detailed measurement of the e^+e^- pair continuum in $p + p$ and Au+Au collisions at $\sqrt{s_{NN}}$ = 200 GeV and implications for direct photon production. Phys.Rev.C 81 (2010), 034911. https://doi.org/10.1103/PhysRevC.81.034911

[9] STAR Collaboration, Dielectron continuum production from $\sqrt{s_{NN}}$ = 200 GeV p + p and Au + Au collisions at STAR. J.Phys.G 38 (2011), 124134. https://doi.org/10.1088/0954-3899/38/12/124134

[10] STAR Collaboration, Measurements of Dielectron Production in Au+Au Collisions at $\sqrt{s_{\rm NN}}$ = 200 GeV from the STAR Experiment. Phys.Rev.C 92 (2015) 2, 024912. https://doi.org/10.1103/PhysRevC.92.024912

[11] Yuanjie Ren, Study of the η to π^0 Ratio in Heavy-Ion Collisions. Phys.Rev.C 104 (2021) 5, 054902. https://doi.org/10.1103/PhysRevC.104.054902

[12] Jia Chen, Nonequilibrium kinetic freeze-out properties in relativistic heavy ion collisions from energies employed at the RHIC beam energy scan to those available at the LHC. Phys.Rev.C 104 (2021) 3, 034901. https://doi.org/10.1103/PhysRevC.104.034901

[13] PHENIX Collaboration, Nonprompt direct-photon production in Au+Au collisions at $\sqrt{s_{NN}}$=200 GeV. Phys.Rev.C 109 (2024) 4, 044912. https://doi.org/10.1103/PhysRevC.109.044912

[14] Jean-François Paquet, Production of photons in relativistic heavy-ion collisions. Phys.Rev.C 93 (2016) 4, 044906. https://doi.org/10.1103/PhysRevC.93.044906

[15] PHENIX Collaboration, Beam Energy and Centrality Dependence of Direct-Photon Emission from Ultrarelativistic Heavy-Ion Collisions. Phys.Rev.Lett. 123 (2019) 2, 022301. https://doi.org/10.1103/PhysRevLett.123.022301

[16] ALICE Collaboration, Measurements of direct-photon production in Pb–Pb collisions at $\sqrt{s_{NN}}$= 5.02 TeV and $\sqrt{s_{NN}}$= 2.76 TeV with the ALICE experiment. PoS HardProbes2023 (2024), 061. https://doi.org/10.22323/1.438.0061

[17] PHENIX Collaboration, Low-$p_{\rm T}$ direct-photon production in Au+Au collisions at $\sqrt{s_{NN}}$=39 and 62.4 GeV. Phys.Rev.C 107 (2023) 2, 024914. https://doi.org/10.1103/PhysRevC.107.024914

[18] ALICE Collaboration, Dielectron production in central Pb−Pb collisions at $\sqrt{s_{\rm NN}}$ = 5.02 TeV. arXiv:2308.16704 [nucl-ex]. https://arxiv.org/abs/2308.16704